BULLETIN *of the*
Malaysian Mathematical
Sciences Society
http://math.usm.my/bulletin

Bull. Malays. Math. Sci. Soc. (2) **28***(2) (2005), 163–172*

Numerical Solution of Boussinesq Equations as a Model of Interfacial-wave Propagation

L.H. Wiryanto
Department of Mathematics, Institut Teknologi Bandung
Jalan Ganesha 10 Bandung, Indonesia
leo@dns.math.itb.ac.id

Abstract. A model of interfacial-wave propagation is solved numerically based on one-dimensional time domain Boussinesq equations, using a predictor-corrector method. The numerical procedure is able to show the effect of non-linearity of the model by observing the wave speed of solitary waves. The procedure is then used to simulate the wave propagation generated, on the left boundary, by a sinusoidal function.

2000 Mathematics Subject Classification: 76B07 (76B55)

Key words and phrases: Boussinesq equations, interfacial wave, predictor-corrector method.

1. Introduction

The existence of a class of nonlinear waves in a density-stratified medium has been demonstrated by several investigators, such as Benney [1], Benjamin [2], Ono [6], and Kubota, Ko & Dobbs [5]. They derived a single equation differently as the model of their internal waves. For two fluid system Segur & Hammack [7] and Choi & Camassa [3] derived the model of the interfacial waves in a KdV-type equation. Another model describing the interfacial waves is Boussinesq type. The derivation of the model can be seen in Grimshaw & Pudjaprasetya [4] who use Hamiltonian formulation.

Most of the equations were then solved analytically to describe solitary waves. Numerical solutions of the equations are an alternative way to observe the wave propagation. Wiryanto [8] solved the KdV equation for the interfacial wave by finite difference method. The procedure was able to simulate the wave propagation in one direction and its deformation at the interface that can be explained as a class of one-direction waves from the model of Boussinesq type.

In this paper the propagation of the interfacial waves is observed numerically from the model of Boussinesq equations. This numerical approach is able to show the propagation for more general type of waves than just solitary, such as sinusoidal. The procedure is constructed by predictor-corrector method, and will be used to

Received: October 11, 2004; *Revised:* March 16, 2005.

show the characteristic such as in analytical works of solitary waves, i.e. the wave breaks up into two, and each wave propagates in different direction. Meanwhile, to preserve the solitary wave propagates in one direction, it is required a relation for the initial elevation and velocity. In linear case, the coefficient q_c is determined quantitatively, and it is larger than the result from the analytical formulation as the nonlinear effect of Boussinesq equations. The wave speed corresponding to the one-direction wave is another quantity that can be determined following q_c.

In presenting this paper, we first describe the Boussinesq equations as the model of interfacial wave in section 2. To provide the condition of one-direction wave, we derive the relation between the elevation and velocity based on depth average in section 3. In the next section, details of the numerical procedure are given, and followed by presenting the numerical computations in section 5. All described in this paper is finally concluded in section 6.

2. Boussinesq equations

The problem is the motion of gravity wave at the interface of two-fluid system having different density ρ_1 for the upper fluid and ρ_2 for the lower fluid as shown in Figure 1. Note that we then use variables with subscribe 1 for the upper fluid and subscribe 2 for the lower fluid. In the undisturbed fluids, the depth of each layer is h_1 and h_2 measured from the interface that is chosen as the horizontal x-axis. Therefore the interfacial wave is presented as the elevation of the interfacial $y(x,t)$ from the undisturbed level, where t is as the time variable. Meanwhile, the fluid system is bounded above and bellow by flat plane.

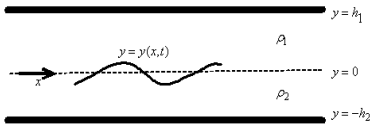

Figure 1. Sketch of the coordinates

The fluids are assumed to be incompressible and inviscid, and the flow is irrotational. This allows us to formulate the problem in potential functions ϕ_1 and ϕ_2 satisfying Laplace equation

$$\bigtriangledown^2\phi_i = 0 \qquad \text{for} \quad i = 1,2 \tag{2.1}$$

in each fluid domain, the kinematics conditions

$$\phi_{1x} = 0 \qquad \text{on} \qquad y = h_1 \tag{2.2}$$

$$\phi_{2x} = 0 \qquad \text{on} \qquad y = -h_2 \tag{2.3}$$

$$y_t + \phi_{ix} y_x = \phi_{ix} \qquad \text{on} \qquad y = y(x,t) \tag{2.4}$$

from upper and lower fluids, and dynamic condition on the interface

$$\rho_1 \left\{ \phi_{1t} + \frac{1}{2}(\phi_{1x}^2 + \phi_{1y}^2) + gy \right\} = \rho_2 \left\{ \phi_{2t} + \frac{1}{2}(\phi_{2x}^2 + \phi_{2y}^2) + gy \right\} \tag{2.5}$$

Equation (2.1) followed (2.2)-(2.5) is approximated into the Boussinesq equations for the interfacial wave as derived in [4],

$$\left.\begin{aligned} u_t + g(\rho_1 - \rho_2)y_x + 2\nu u u_x &= 0 \\ y_t + \tfrac{h_1 h_2}{\rho_1 h_2 + \rho_2 h_1} u_x + 2\nu(yu)_x + 2\beta u_{xxx} &= 0 \end{aligned}\right\} \tag{2.6}$$

where g is acceleration due to gravity,

$$\nu = \frac{1}{2}\frac{\rho_2 h_1^2 - \rho_1 h_2^2}{(\rho_1 h_2 + \rho_2 h_1)^2}, \quad \beta = \frac{h_1^2 h_2^2}{6}\frac{\rho_1 h_1 + \rho_2 h_2}{(\rho_1 h_2 + \rho_2 h_1)^2} \tag{2.7}$$

and u is defined as

$$u = (\rho_2\phi_2 - \rho_1\phi_1)_x \qquad \text{on} \quad y = y(x,t). \tag{2.8}$$

For convenience, Equation (2.6) is non-dimensionalized by taking h_1 as the unity of length and $\sqrt{gh_1}$ as the unity of speed. Therefore two parameters involved in the equations are

$$h = \frac{h_2}{h_1}, \quad \rho = \frac{\rho_2}{\rho_1}. \tag{2.9}$$

The equations are then written in normalized variables which will show the dominating terms in the equations, by defining

$$\eta = \frac{y}{a}, \;\; \xi = x\sqrt{a}, \;\; \tau = t\sqrt{a}, \;\; \vartheta = \frac{u}{a} \tag{2.10}$$

where a is a reference value of y such as the order of amplitude. These transform (2.6) to the form

$$\vartheta_\tau + \left((\rho - 1)\eta + \frac{a(\rho - h^2)}{2(h+\rho)^2}\vartheta\right)_\xi = 0 \tag{2.11}$$

$$\eta_\tau + \left(\frac{h}{\rho + h}\vartheta + \frac{a(\rho - h^2)}{(h+\rho)^2}\eta\vartheta + \frac{h^2 a(\rho h + 1)}{3(\rho + h)^2}\vartheta_{\xi\xi}\right)_\xi = 0 \tag{2.12}$$

For small a, (2.11) and (2.12) can be reduced to a simple wave equation of ϑ or η by eliminating one of both unknowns, and can be solved analytically by separating the independent variable. On the other hand, the effect of the nonlinear and third derivative terms will be observed by solving (2.11) and (2.12) numerically.

3. One-direction wave

Equations (2.11) and (2.12) are able to explain wave propagation in two directions. In special relation of the initial conditions ϑ and η, the equations give a wave travelling only in one direction. We derive that relation by considering the depth-average horizontal velocity defined as

$$\bar{\phi}_{1x} = \frac{1}{1 - a\eta}\int_{a\eta}^{1} \phi_{1x}\, dy \qquad \text{for the upper fluid} \tag{3.1}$$

$$\bar{\phi}_{2x} = \frac{1}{h + a\eta}\int_{-h}^{a\eta} \phi_{2x}\, dy \qquad \text{for the lower fluid} \tag{3.2}$$

in non-dimensional variables corresponding to (2.10).

The integration in (3.1) and (3.2) can be expressed in η derived as followed. For the lower fluid, we start from Laplace equation (2.1) integrated on the thickness of the lower fluid

$$\int_{-h}^{a\eta} a\phi_{2xx} + \phi_{2yy}\, dy = 0. \tag{3.3}$$

From the kinematics conditions (2.3) and (2.4), and relation

$$\frac{\partial}{\partial x}\int_{-h}^{a\eta} \phi_{2x}\, dy = a\, \phi_{2x}|_{a\eta}\, \eta_x + \int_{-h}^{a\eta} \phi_{2xx}\, dy \tag{3.4}$$

(3.3) becomes

$$\frac{\partial}{\partial x}\int_{-h}^{a\eta} \phi_{2x}\, dy + \eta_t = 0. \tag{3.5}$$

The next step, we suppose that the wave travels to the right. This is expressed in η as

$$\eta_t + c\eta_x = 0 \tag{3.6}$$

with wave speed

$$c = \sqrt{\frac{h(\rho-1)}{h+\rho}} \tag{3.7}$$

obtained from the leading order of (2.11) and (2.12). We then substitute (3.6) to (3.5), and integrate with respect to x, giving

$$\int_{-h}^{a\eta} \phi_{2x}\, dy = c\eta \tag{3.8}$$

The constant of integration is zero as η, $\phi_{2x} \to 0$ for $|x| \to \infty$. Relation (3.8) is then used to eliminate the integral in (3.2), so that we have

$$\bar{\phi_2}_x = \frac{c\eta}{h+a\eta}. \tag{3.9}$$

When the above procedure is followed for the upper fluid, (13) becomes

$$\bar{\phi_1}_x = \frac{c\eta}{a\eta-1}. \tag{3.10}$$

Results (3.9) and (3.10) are used to approximate u in Boussinesq equations to obtain one-direction traveling wave, i.e.

$$u \approx \left(\frac{\rho}{h+a\eta} - \frac{1}{a\eta-1}\right) c\eta. \tag{3.11}$$

4. Numerical procedure

In investigating the propagation of the interfacial waves, the model in form of Boussinesq equations is solved numerically. A numerical procedure is developed for (2.11) and (2.12). A predictor-corrector method is chosen as it can be applied to the equations explicitly. To simplify in explaining the method, (2.11) and (2.12) are expressed in form

$$\vartheta_\tau = F(\eta, \vartheta)$$
$$\eta_\tau = G(\eta, \vartheta)$$

where

$$F(\eta,\vartheta) = -\left((\rho-1)\eta + \frac{a(\rho-h^2)}{2(h+\rho)^2}\vartheta^2\right)_\xi \tag{4.1}$$

$$G(\eta,\vartheta) = -\left(\frac{h}{\rho+h}\vartheta + \frac{a(\rho-h^2)}{(h+\rho^2)}\eta\vartheta + \frac{h^2a(\rho h+1)}{3(\rho+h)^2}\vartheta_{\xi\xi}\right)_\xi . \tag{4.2}$$

The equations are finite-differenced on a grid in ξ and τ. The discrete independent variables are expressed as $\xi = i\Delta\xi$, $\tau = n\Delta\tau$ with level n referring to information at the present, known time level. The predictor step is the third-order explicit Adam-Bashforth scheme given by

$$\vartheta_i^{n+1} = \vartheta_i^n + \frac{\Delta\tau}{12}\left[23F_i^n - 16F_i^{n-1} + 5F_i^{n-2}\right] \tag{4.3}$$

$$\eta_i^{n+1} = \eta_i^n + \frac{\Delta\tau}{12}\left[23G_i^n - 16G_i^{n-1} + 5G_i^{n-2}\right] \tag{4.4}$$

The predicted values (4.3) and (4.4) are then used to evaluate F_i^{n+1} and G_i^{n+1} from (4.1) and (4.2) which will be used to correcting ϑ_i^{n+1} and η_i^{n+1} above. The scheme for it is the fourth-order Adams-Moulton method, given by

$$\vartheta_i^{n+1} = \vartheta_i^n + \frac{\Delta\tau}{24}\left[9F_i^{n+1} + 19F_i^n - 5F_i^{n-1} + F_i^{n-2}\right] \tag{4.5}$$

$$\eta_i^{n+1} = \eta_i^n + \frac{\Delta\tau}{24}\left[9G_i^{n+1} + 19G_i^n - 5G_i^{n-1} + G_i^{n-2}\right]. \tag{4.6}$$

This scheme is also calculated explicitly.

In running the numerical procedure, the predictor step requests two previous time levels at $n-1$ and $n-2$. This must be treated specially at $n = 0$ and 1 as we need values before the initial ones. This problem can be solved by defining the same value at the initial condition.

Another problem is boundary conditions and some values of ϑ_i^n and η_i^n outside the observation domain. We suppose to observe the wave propagation in $\xi \in [0, L]$ and we discretize as

$$\xi_i = i\Delta\xi, \qquad \Delta\xi = \frac{L}{M}, \qquad i = 0, 1, 2, \cdots, M.$$

Table 1. Data of the left-going wave (a) and the right-going wave (b).

t	x	a_m
24.64147	57.24334	0.07345
26.87754	56.34891	0.07328
29.11360	55.45449	0.07311
31.34967	54.56006	0.07294
33.58574	53.66563	0.07278
35.82181	52.77120	0.07261
38.05788	51.87678	0.07244
40.29394	50.98235	0.07227

(a)

t	x	a_m
24.64147	76.92074	0.07345
26.87754	77.81517	0.07328
29.11360	78.70959	0.07311
31.34967	79.60402	0.07294
33.58574	80.49845	0.07278
35.82181	81.39288	0.07261
38.05788	82.28730	0.07244
40.29394	83.18173	0.07227

(b)

The finite difference for the derivative (up to third) of ϑ and η in the observation domain needs values from $i = -2$ to $i = M+2$. As the values outside the domain are provided every time level n, we can overcome this problem by linearizing those values of both ϑ and η to the values in the domain. This can be done as the assumption that the domain is relatively long so that the boundary gives very small effect and can be neglected to the wave which is propagating far from the boundary.

5. Numerical results

The numerical procedure described in the previous section is used to observe the propagation of interfacial waves for various initial values $\vartheta(\xi, 0)$ and $\eta(\xi, 0)$. Most results presented here are obtained from calculation using $\Delta\xi = 0.1$, $\Delta\tau = 0.02$, $a = 0.1$; and waves are plotted in non-dimensional variables y versus x. The propagation and deformation of waves are shown by plotting the result of calculation at some time levels t in the same coordinates, but we shift the values y upper for higher time levels.

Figure 2 is typical interfacial waves when the initial conditions are solitary in the form

$$y(x, 0) = A \operatorname{sech}^2[b(x - xo)] \tag{5.1}$$

for constants A, b, xo, and the horizontal velocity $u = 0$. The plot is the numerical result for quantities $h = 0.8$, $\rho = 1.5$, and $A = 0.15$, $b = 1.0$, $xo = 67.08$. From the calculation we found that the solitary wave breaks up into two, and then each wave travels in different direction. The amplitude and the wave speed are calculated from Table 1a representing time t, position of wave peak x and the amplitude a_m at that time for the left-going wave, and Table 1b for the other wave. We present the data for the last 8 curves as shown in Figure 2 where the initial wave has broken up into two waves.

The third column of both tables indicates that the both waves have same amplitude, but it decreases by increasing time. Our calculation shows that up to $t = 40.29394$ the maximum height reaches 0.0722. Meanwhile, plot of the first column versus second one produces a line $x = -0.4t + 67.1$ for Table 1a, and $x = 0.4t + 67.06$ for Table 1b. These are the position of the wave peak at time t.

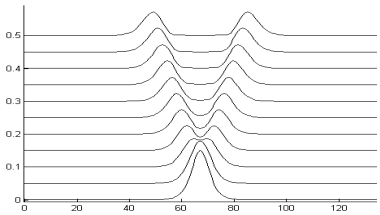

Figure 2. Propagation of interfacial wave $y(x,0) = 0.15\ \mathrm{sech}^2(x - 67.08)$, $u(x,0) = 0$ for $h = 0.8$, $\rho = 1.5$

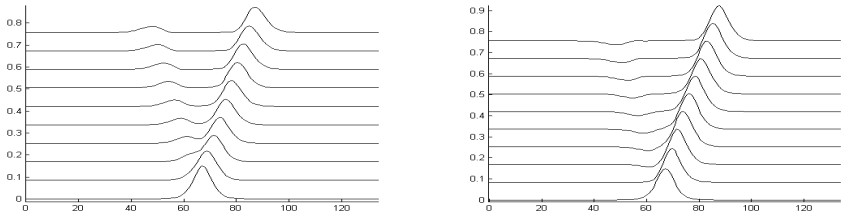

(a) (b)

Figure 3. Propagation of wave for $h = 0.8$, $\rho = 1.5$ with (a) $u(x,0) = 0.7\ y(x,0)$, (b) $u(x,0) = 1.5\ y(x,0)$

The coefficient of the line represents the wave speed, i.e. both waves have the same wave speed 0.4. The negative sign indicates left direction.

Now when the above initial solitary wave is followed by $u(x,0) = q\ y(x,0)$, with constant q, the wave will break up into two having different amplitude. Figure 3a shows the wave deformation for $q = 0.7$. The right-going wave has wave speed $c_R = 0.446$ and amplitude 0.115. Meanwhile the other wave has wave speed $c_L = -0.400$ and amplitude 0.029. For larger q the left-going wave has smaller amplitude, and $q_c = 1.183$ is the critical value where no left-going wave. This critical value is different with the coefficient of the linearized of (3.11), i.e. 1.199, since we solve the Boussinesq equations involving the nonlinear terms. Therefore, the difference is the corrector factor of the linearized (3.11). For $q > q_c$ the left-going wave appears with negative amplitude. We show this in Figure 3b for $q = 1.5$.

In comparison with the KdV-type equation, we found that the numerical solution of Boussinesq equations can explain the character in KdV equation by setting $u(x,0) = q_c\ y(x,0)$. For solitary waves deforming to some solitons, our procedure is able to show them using the initial elevation as given in (5.1) for a suitable value b with respect to the amplitude. Figure 4a shows a solitary wave deforming to two solitons. We obtain that result as the solution of Bossinesq equations using initial condition

$$y(x,0) = 0.4\ \mathrm{sech}^2[0.5(x - 10.0)]$$
$$u(x,0) = 1.183\ y(x,0)$$

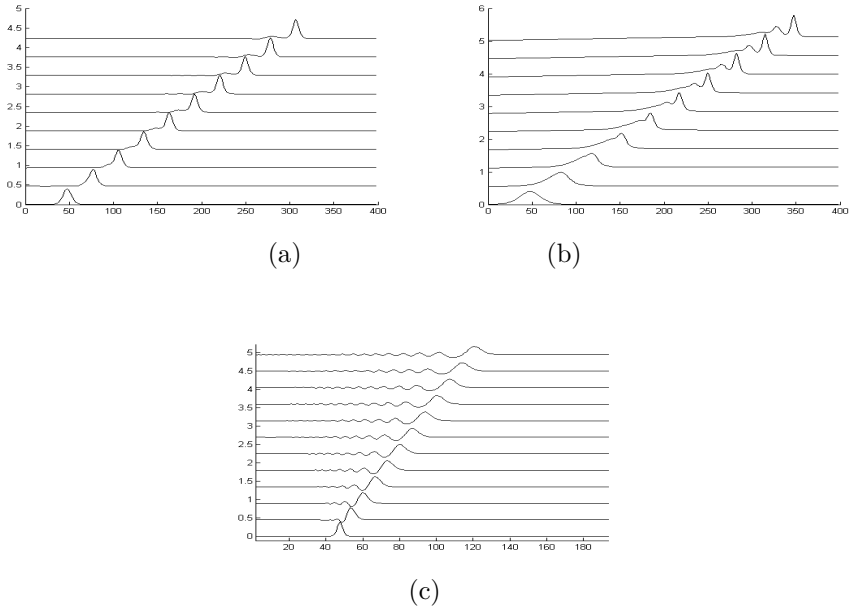

Figure 4. Wave deformation from solitary to two solitons (a), three solitons (b), and appearing a train of waves (c).

Table 2. The critical value q_c and wave speed c for various h and ρ.

$\rho = 1.2$

h	q_c	c
0.5	0.81	0.265
0.6	0.756	0.274
0.7	0.724	0.276
0.8	0.701	0.277

(a)

$\rho = 1.5$

h	q_c	c
0.6	1.290	0.400
0.7	1.226	0.406
0.8	1.183	0.427
0.9	1.148	0.320

(b)

and parameters $h = 0.8$, $\rho = 1.5$. For smaller values b the initial solitary wave can deforms to more solitons, and larger values b a train of small waves appears behind the main solitary. We show these in Figure 4b and 4c, corresponding to $b = 0.2$ and $b = 1.7$ respectively.

For other values h and ρ, the critical value q_c was determined as described above. The corresponding wave propagates to the right with wave speed c as given in Table 2. The amplitude of the wave was observed during propagating and we found that it is relatively constant around $a_m = 0.150$. For larger values h, our numerical procedure is not able to give smooth waves, since this increases the coefficient of $\vartheta_{\xi\xi\xi}$ in (12), and this term dominates the equation.

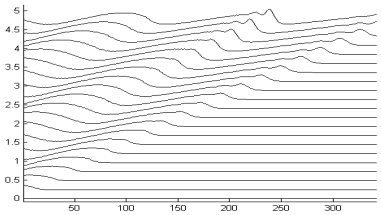

Figure 5. Sinusoidal waves generated on the left as the boundary and propagating along the interface.

Figure 5 shows the propagation of a typical sinusoidal wave coming in the observation domain having $\rho = 1.5$ and $h = 0.8$. At the beginning the interface is undisturbed, and the left boundary is assumed to be a wave generator with

$$y(0,t) = 0.15\sin(ct)$$

$$u(0,t) = \left(\frac{\rho}{y(0,t)+h} - \frac{1}{y(0,t)-1}\right) cy(0,t)$$

where c is the incoming wave speed defined in (3.7). From our calculation, we obtained that the elevation of the interface forms waves propagating to the right, and deformation occurs as shown in Figure 5. The crest of the sinusoidal deforms to solitary-like wave and breaks to two waves. This is also obtained from the KdV model, see [8].

6. Conclusions

Numerical solutions of Boussinesq equations for interfacial wave have been presented. The model was solved by a predictor-corrector method. We demonstrated the solutions as the wave propagation for typical solitary and sinusoidal. The initial condition of the horizontal velocity plays an important role in observing the wave deformation, mainly break up to two waves travelling in different direction. In case where the initial velocity u is linear to the initial elevation, we found that the wave travels only in one direction for a certain value of the coefficient q_c of that linear relation. The class of these one-direction waves can explain the character of solutions in KdV model. The non-linear effect of Boussinesq equations is shown in values q_c and wave speed c which are different from the linearized (3.11) and (3.7) for various h and ρ.

Acknowledgment. The research of this report was supported by QUE (quality undergraduate education) project for Mathematics Institut Teknologi Bandung. The author thanks Dr. Pudjaprasetya for stimulating discussions.

References

[1] D. J. Benney, Long nonlinear waves in fluid flows, *J. Math. Physics.* **45** (1966), 52–63.
[2] T. B. Benjamin, Internal waves of permanent form in fluids of great depth, *J. Fluid Mech.* **29** (1967), 559–592.

[3] W. Choi and R. Camassa, Weakly nonlinear internal waves in a two-fluid system, *J. Fluid Mech.* **313** (1996), 83–103.
[4] R. Grimshaw and S.R. Pudjaprasetya, Hamiltonian formulation for the description of interfacial solitary waves, *Nonlinear processes in geophysics* **5** (1998), 3–12.
[5] T. Kubota, D. R. S. Ko, and L. D. Dobbs, Weakly-nonlinear, long internal gravity waves in stratified fluids of finite depth, *J. Hydronoutics* (1978), 157–165.
[6] H. Ono, Algebraic solitary wave in stratified fluids, *J. Phys. Soc. Japan* **39** (1975), 1082–1091.
[7] H. Segur and J. L. Hammack, Soliton models of long internal waves, *J. Fluid Mech.* **118** (1982), 285–304.
[8] L. H. Wiryanto, A finite difference method on KdV equation of internal waves, (in preparation).